Mendeleev Communications

*Mendeleev Commun.*, 2025, **35**, 90–92

# Synthesis of MXene/$TiO_2$ heterostructures for enhanced photocatalytic $CO_2$ reduction under visible light

**Anna Yu. Kurenkova,[a] Danila B. Vasilchenko,[a,b] Andrey A. Saraev,[a,c] Roman F. Alekseev,[a] Egor E. Aydakov,[a] Denis D. Mishchenko,[a,c] Evgeny Yu. Gerasimov[a] and Ekaterina A. Kozlova*[a]**

[a] *G. K. Boreskov Institute of Catalysis, Siberian Branch of the Russian Academy of Sciences, 630090 Novosibirsk, Russian Federation. E-mail: kozlova@catalysis.ru*
[b] *A. V. Nikolaev Institute of Inorganic Chemistry, Siberian Branch of the Russian Academy of Sciences, 630090 Novosibirsk, Russian Federation*
[c] *Synchrotron Radiation Facility 'SKIF', Boreskov Institute of Catalysis, Siberian Branch of the Russian Academy of Sciences, 630559 Kol'tsovo, Novosibirsk Region, Russian Federation*

DOI: 10.71267/mencom.7588

**The modification of $TiO_2$-based photocatalysts with 5 wt% $Ti_3C_2$ (MXene) enhanced the reaction rate of $CO_2$ reduction by a factor of 2.8. The MXene $Ti_3C_2$ is an effective cocatalyst for $CO_2$ reduction to $CH_4$ under visible light irradiation (400 nm).**

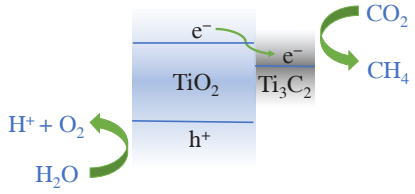


*Keywords*: photocatalysis, photocatalysts, MXenes, titanium carbide, $Ti_3C_2$, titanium dioxide, $TiO_2$, photocatalytic $CO_2$ reduction.

The current trend towards carbon footprint reduction and growing energy consumption requires the creation of new or modernization of existing energy production systems. This concept includes, among other things, development of renewable energy sources, reduction of greenhouse gas emissions, and improvement of energy efficiency.[1,2] The reduction of $CO_2$ with the formation of $CH_4$, CO, $CH_3OH$, HCHO, HCOOH, $C_2H_5OH$, *etc*., is of great interest not only for obtaining solar fuel and intermediates for the chemical industry but also for reducing the greenhouse effect.[3–5]

The main factor restraining the practical use of photocatalytic conversion of $CO_2$ is the lack of efficient heterogeneous photocatalysts functioning under the action of sunlight.[6] This is largely due to the weak absorption of irradiation in the visible region by photocatalysts and recombination of photogenerated charge carriers.[7] The creation of composite materials based on a stable and safe material, titanium dioxide ($TiO_2$), widely used as a photocatalyst, can solve the above problems.[8] Promising cocatalysts that improve the activity of bulk $TiO_2$ are various

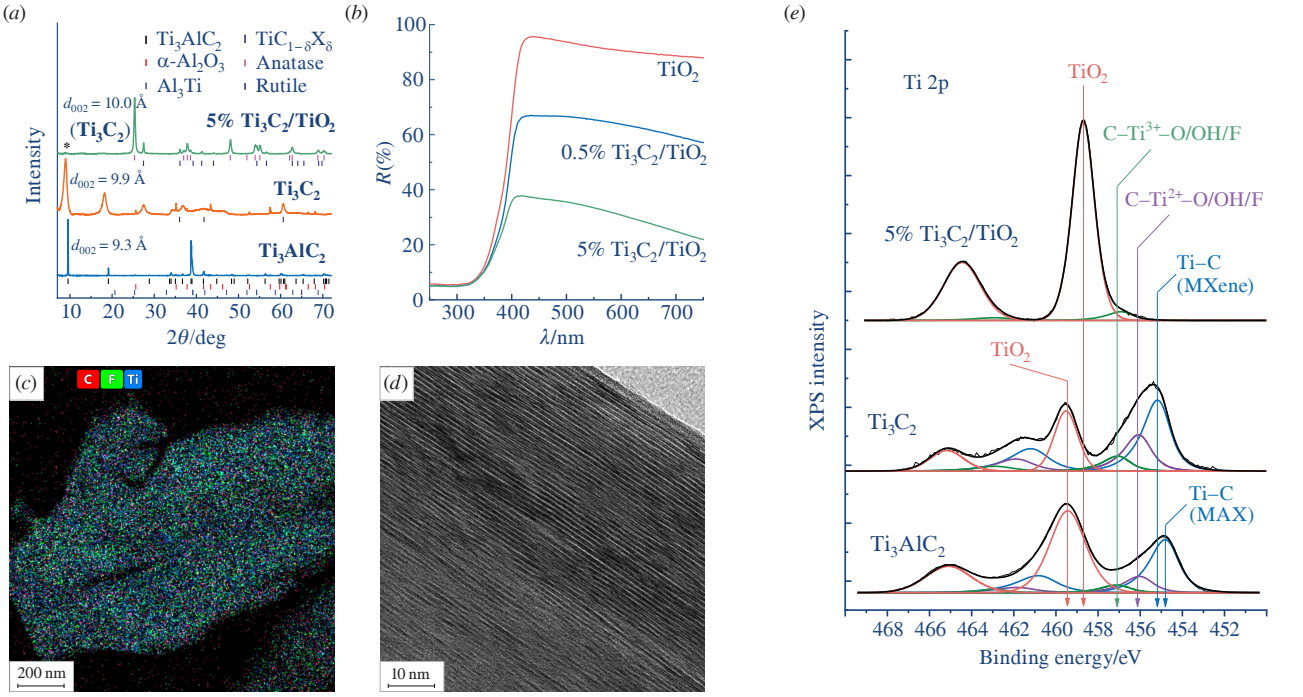


**Figure 1** (*a*) XRD patterns of $Ti_3AlC_2$, $Ti_3C_2$, and 5% $Ti_3C_2/TiO_2$; (*b*) diffuse reflectance spectra of $TiO_2$, 0.5% $Ti_3C_2/TiO_2$, and 5% $Ti_3C_2/TiO_2$; (*c*) EDX mapping and (*d*) HRTEM image of $Ti_3C_2$; and (*e*) Ti 2p core-level spectra of $Ti_3AlC_2$, $Ti_3C_2$, and 5% $Ti_3C_2/TiO_2$.

2D layered materials such as $MoS_2$,[9] g-$C_3N_4$,[10] h-BN,[11] borophene,[12] and black phosphorous.[13] These 2D materials attract enormous attention due to their unique electronic and catalytic properties.[6] MXenes, a new type of 2D transition metal carbides ($M_{n+1}C_n$, $n$ = 1, 2, or 3), attracted much attention since the synthesis of 2D $Ti_3C_2$ in 2011.[14,15] $Ti_3C_2$ MXenes have great prospects for use in photocatalysis due to their large specific surface area, high electrical conductivity, narrow band gap, and the possibility of surface functionalization by the introduction of terminal groups (–OH, –F, *etc.*).[3] Recently, $Ti_3C_2/TiO_2$ composites have been synthesized for photocatalytic carbon dioxide reduction,[2] hydrogen production,[16] and nitrogen photofixation.[17]

We synthesized 0.5–5 wt% $Ti_3C_2/TiO_2$ photocatalysts based on robust commercial $TiO_2$ Evonik P25 (anatase/rutile) for photocatalytic $CO_2$ reduction under visible light and determined the effect of MXene loading on the overall rate of carbon dioxide reduction and on selectivity for methane and carbon monoxide.

The synthesis of $Ti_3C_2$ MXenes was performed by classical etching of MAX phase $Ti_3AlC_2$ in an aqueous solution of LiF/HCl. The deposition of $Ti_3C_2$ on the surface of P25 was carried out in a water suspension of MXene $Ti_3C_2$ and $TiO_2$. The synthesized samples and starting $TiO_2$ P25 were characterized by XRD analysis, UV-Vis spectroscopy, HRTEM with EDX analysis, and XPS (see Online Supplementary Materials for details). Figure 1 represents XRD patterns and UV-Vis and XPS spectra of a precursor MAX phase ($Ti_3AlC_2$), MXene ($Ti_3C_2$), and a 5% $Ti_3C_2/TiO_2$ sample. According to XRD analysis, the precursor sample contained two MAX phases: (1) $Ti_3AlC_2$ with structural parameters close to published data[18] and (2) $Ti_3AlC_2$, which had a predominant orientation along the (002), (004), and (008) planes and an increased crystalline size; α-$Al_2O_3$ and $Al_3Ti$ impurities were also found (Table S1). The XRD patterns of $Ti_3C_2$ are typical for MXenes.[16] The MXene lattice was strongly distorted compared to that of the MAX phase, but the shift of the first peak corresponded to the (002) diffraction plane to lower angles could be attributed to the removal of Al from the MAX phase.[2] Another evidence of the formation of MXene was the presence of a so-called hk-band (unresolved diffraction band) in the region of $2\theta \approx 33.6–49.4°$. The impurity $Al_2O_3$ phase remained unchanged after MXene formation, whereas the $Al_3Ti$ phase disappeared (Table S1). For the composite 5 wt% $Ti_3C_2/TiO_2$ sample, observed peaks of anatase and rutile corresponded to $TiO_2$ P25;[15] a low intensity peak at 10.1° corresponded to the interplanar distance (002) of $Ti_3C_2$ MXene. The deposition of MXenes also changed the textural properties of the photocatalyst. In composite photocatalysts, the specific surface area decreased compared to the $TiO_2$ P25, but the pore volume increased (Table S2). The UV-Vis spectra of $TiO_2$ P25 and 0.5–5 wt% $Ti_3C_2/TiO_2$ samples are presented in Figure 1(*b*); the band gap energy ($E_g$) was calculated using a Tauc plot for indirect allowed transition (Table 1). The absorption in the visible range increased with the $Ti_3C_2$ content from 0.5 to 5 wt%, whereas the band gap energy slightly decreased from 3.01 eV for pristine P25 to 2.87 eV for 5 wt% $Ti_3C_2/TiO_2$. The TEM images of MXene ($Ti_3C_2$) confirmed uniform distribution of Ti, C, and F on the surface of MXene [Figure 1(*c*)]; EDX analysis (Table S3) showed the predominant content of titanium and carbon, and the

**Table 1** Properties and activity of 0.5 and 5 wt% $Ti_3C_2/TiO_2$ photocatalysts and commercial $TiO_2$ P25 in carbon dioxide reduction. Conditions: 101 kPa $CO_2$ with saturated water vapor, $m$(cat) = 30 mg, 400-nm LED irradiation.

| Entry | Sample | $E_g$/eV | $v$/μmol g$^{-1}$ h$^{-1}$ | | | $v_e$ ($CO_2$)/ μmol g$^{-1}$ h$^{-1}$ |
|---|---|---|---|---|---|---|
| | | | $CH_4$ | CO | $H_2$ | |
| 1 | $TiO_2$ | 3.01 | 0.50 | 1.53 | 0.13 | 7.08 |
| 2 | 0.5% $Ti_3C_2/TiO_2$ | 2.96 | 1.78 | 0.77 | 1.20 | 15.8 |
| 3 | 5% $Ti_3C_2/TiO_2$ | 2.87 | 2.24 | 0.87 | 2.13 | 19.7 |

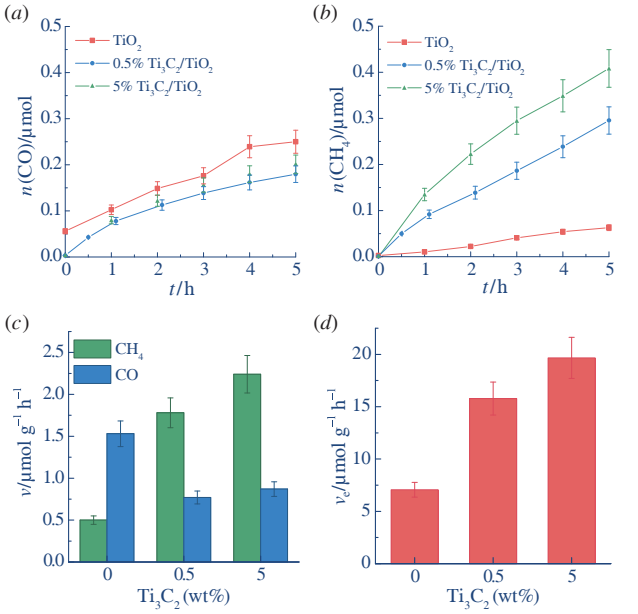


**Figure 2** Kinetic curves of (*a*) CO and (*b*) $CH_4$ production over photocatalysts; (*c*) the rate of product formation, and (*d*) total electron consumption during $CO_2$ reduction.

atomic ratio F/Ti was approximately 1/2, which suggested the formation of $Ti_3C_2F_x$ ($x$ ~ 1.5). Concentrations of Al impurities did not exceed 1 at%. The HRTEM image [Figure 1(*d*)] showed a layered structure of the synthesized MXene, which is typical for this class of materials.[6,15,19] The Ti 2p core-level spectrum of MAX phase [Figure 1(*e*)] was fitted by three Ti $2p_{3/2}$–Ti $2p_{1/2}$ doublets with of Ti $2p_{3/2}$ binding energy peaks at 454.8, 456.1, and 457.1, and 459.5 eV corresponded to Ti–C, C–$Ti^{2+}$, and C–$Ti^{3+}$ with O/OH terminal groups, the fourth peak corresponded to a $TiO_2$ impurity.[20–22] The increased Ti $2p_{3/2}$–Ti $2p_{1/2}$ doublet binding energy corresponded to a $TiO_2$ impurity due to a charge effect of low-conductive phase; moreover, it is likely that $TiO_2$ was an amorphous phase, which could not be detected by XRD. The Ti 2p core-level spectrum of synthesized MXene was fitted by the same components, but the Ti $2p_{3/2}$ binding energy of 455.2 eV corresponded to Ti–C to confirm the formation of MXene.[20–22] Note that etching of a MAX phase in an aqueous solution of LiF/HCl could result in formation of terminal –F groups. The Ti 2p core-level spectrum of 5% $Ti_3C_2/TiO_2$ was fitted by two Ti $2p_{3/2}$–Ti $2p_{1/2}$ doublets with Ti $2p_{3/2}$ binding energy peaks at 457.0 and 458.7 eV due to C–$Ti^{3+}$–F of MXene and $Ti^{4+}$ of $TiO_2$ P25, respectively.

The photocatalytic gas-phase $CO_2$ reduction with $H_2O$ was carried out in a batch reactor under irradiation with a 400-nm LED; the reaction setup (Figure S1) was described elsewhere.[23] CO, $CH_4$, and $H_2$ were identified as the main reaction products (Table 1). Figure 2 shows the kinetic curves of CO and $CH_4$ formation, respectively. The total rate of electrons consumed for photocatalytic $CO_2$ reduction (Table 1) was calculated according to the equation

$$v_e(CO_2) = 8v(CH_4) + 2v(CO), \quad (1)$$

where $v(CH_4)$ and $v$(CO) are the rates of $CH_4$ and CO formation (μmol g$^{-1}$ h$^{-1}$).[18,19] Figures 2(*c*),(*d*) and Table 1 show the rates of product formation and the overall $CO_2$ reduction rate. The conversion of $CO_2$ under exposure to visible light ($\lambda$ = 400 nm) was observed on $TiO_2$ P25 and 0.5–5 wt% $Ti_3C_2/TiO_2$ P25. However, the main reduction product was CO in the case of unmodified $TiO_2$, while $CH_4$ became the predominant product in the case of 0.5% $Ti_3C_2/TiO_2$ P25 and 5% $Ti_3C_2/TiO_2$ P25 photocatalysts. Methane is an important product of $CO_2$ conversion under irradiation with solar light because solar energy

can be stored in synthetic natural gas to be used as an energy carrier. Earlier, we observed a similar pattern when moving from $TiO_2$ to photocatalysts with deposited noble metals like $Pt/TiO_2$, $Ag/TiO_2$, and $CuO_x/TiO_2$.[18,19,24] Obviously, the formation of $CH_4$ rather than CO is thermodynamically more favorable; however, the formation of methane is a complex eight-electron process. For this process to proceed effectively, accumulation of electron density near the surface of metal nanoparticles is required. [18,19] Thus, we can assume that, when $Ti_3C_2$ MXenes were deposited on the surface of titania, the same effect was observed as when $TiO_2$ was doped with metals due to unique properties of MXenes, such as high metal conductivity and the ability to accumulate high electron density.[14] The metallic properties of supported MXenes were indirectly manifested in a large increase in the rate of hydrogen production (see Table 1). Previously, it was found that the deposition of MXene on the surface of $TiO_2$ or other semiconductors increased the selectivity for methane,[3,18] and this was also confirmed by quantum chemical calculations.[25]

It should be noted that the overall rate of $CO_2$ reduction increased with the addition of MXene to $TiO_2$ to reach 19.7 μmol $g^{-1}$ $h^{-1}$ as the weight fraction was increased from 0.5 to 5%. A comparison with recently published data on $CO_2$ reduction over MXene-containing photocatalysts (Table S4) showed that the activity of the 0.5–5 wt% $Ti_3C_2/TiO_2$ photocatalysts was at the same level or higher than the activity of similar systems. A higher activity was obtained when high-power xenon lamps without light filters were used as an irradiation source. Moreover, the activity of $TiO_2$ modified with $Ti_3C_2$ MXene exceeded the activity of platinized $TiO_2$ in photocatalytic $CO_2$ reduction in similar conditions.[23]

Thus, we proposed active 0.5–5 wt% $Ti_3C_2/TiO_2$ photocatalysts for $CO_2$ reduction under visible light with predominant methane formation. The deposition of MXenes on a titania surface had a similar effect to that of the deposition of metal cocatalysts. Note that the composites based on $Ti_3C_2$ MXenes and commercially available $TiO_2$ Evonik P25 were prepared for the first time for the $CO_2$ reduction process using simple synthetic approaches.

This work was supported by the Russian Science Foundation (grant no. 24-13-00416).

*Online Supplementary Materials*

Supplementary data associated with this article can be found in the online version at doi: 10.71267/mencom.7588.

## References

1 R. F. Alekseev, A. A. Saraev, A. Yu. Kurenkova and E. A. Kozlova, *Russ. Chem. Rev.*, 2024, **93**, 5124; https://doi.org/10.59761/RCR5124.

2 S. G. Zlotin, K. S. Egorova, V. P. Ananikov, A. A. Akulov, M. V. Varaksin, O. N. Chupakhin, V. N. Charushin, K. P. Bryliakov, A. D. Averin, I. P. Beletskaya, E. L. Dolengovski, Y. H. Budnikova, O. G. Sinyashin, Z. N. Gafurov, A. O. Kantyukov, D. G. Yakhvarov, A. V. Aksenov, M. N. Elinson, V. G. Nenajdenko, A. M. Chibiryaev, N. S. Nesterov, E. A. Kozlova, O. N. Martyanov, I. A. Balova, V. N. Sorokoumov, D. A. Guk, E. K. Beloglazkina, D. A. Lemenovskii, I. Y. Chukicheva, L. L. Frolova, E. S. Izmest'ev, I. A. Dvornikova, A. V. Popov, A. V. Kutchin, D. M. Borisova, A. A. Kalinina, A. M. Muzafarov, I. V. Kuchurov, A. L. Maximov and A. V. Zolotukhina, *Russ. Chem. Rev.*, 2023, **92**, 5104; https://doi.org/10.59761/RCR5104.

3 Y. Zheng, Z. Li, Q. Li, E. Liu, D. Liu, Y. Liang, B. Han, J. Qi, G. Wei and L. Zhu, *Sep. Purif. Technol.*, 2024, **347**, 127591; https://doi.org/10.1016/j.seppur.2024.127591.

4 K. C. Devarayapalli, B. Kim, A. R. Manchuri, Y. Lim, G. Kim and D. S. Lee, *Appl. Surf. Sci.*, 2023, **636**, 157865; https://doi.org/10.1016/j.apsusc.2023.157865.

5 V. N. Borshch, S. Ya. Zhuk, E. V. Pugacheva, T. D. Dipheko, D. E. Andreev, Yu. A. Agafonov and O. L. Eliseev, *Mendeleev Commun.*, 2023, **33**, 55; https://doi.org/10.1016/j.mencom.2023.01.017.

6 E. A. Kozlova, M. N. Lyulyukin, D. V. Kozlov and V. N. Parmon, *Russ. Chem. Rev.*, 2021, **90**, 1520; https://doi.org/10.1070/RCR5004.

7 H.-E. Nemamcha, N.-N. Vu, D. S. Tran, C. Boisvert, D. D. Nguyen and P. Nguyen-Tri, *Sci. Total Environ.*, 2024, **931**, 172816; https://doi.org/10.1016/j.scitotenv.2024.172816.

8 L. Biswal, R. Mohanty, S. Nayak and K. Parida, *J. Environ. Chem. Eng.*, 2022, **10**, 107211; https://doi.org/10.1016/j.jece.2022.107211.

9 G. Swain, S. Sultana and K. Parida, *ACS Sustainable Chem. Eng.*, 2020, **8**, 4848; https://doi.org/10.1021/acssuschemeng.9b07821.

10 A. V. Zhurenok, D. B. Vasilchenko and E. A. Kozlova, *Int. J. Mol. Sci.*, 2023, **24**, 346; https://doi.org/10.3390/ijms24010346.

11 L. Acharya, S. Nayak, S. P. Pattnaik, R. Acharya and K. Parida, *J. Colloid Interface Sci.*, 2020, **566**, 211; https://doi.org/10.1016/j.jcis.2020.01.074.

12 Z. Zhang, Y. Yang, E. S. Penev and B. I. Yakobson, *Adv. Funct. Mater.*, 2017, **27**, 1605059; https://doi.org/10.1002/adfm.201605059.

13 A. M. Kuchkaev, A. V. Zhurenok, A. M. Kuchkaev, A. V. Sukhov, V. S. Kashansky, M. M. Nikitin, K. A. Litvintseva, S. V. Cherepanova, E. Yu. Gerasimov, E. A. Kozlova, O. G. Sinyashin and D. G. Yakhvarov, *Kinet. Catal*., 2024, **65**, 513; https://doi.org/10.1134/S0023158424601979.

14 M. Naguib, M. Kurtoglu, V. Presser, J. Lu, J. Niu, M. Heon, L. Hultman, Y. Gogotsi and M. W. Barsoum, *Adv. Mater.*, 2011, **23**, 4248; https://doi.org/10.1002/adma.201102306.

15 Z. Otgonbayar and W.-C. Oh, *Mol. Catal.*, 2023, **541**, 113085; https://doi.org/10.1016/j.mcat.2023.113085.

16 T. Su, Z. D. Hood, M. Naguib, L. Bai, S. Luo, C. M. Rouleau, I. N. Ivanov, H. Ji, Z. Qin and Z. Wu, *ACS Appl. Energy Mater.*, 2019, **2**, 4640; https://doi.org/10.1021/acsaem.8b02268.

17 Y. Liao, J. Qian, G. Xie, Q. Han, W. Dang, Y. Wang, L. Lv, S. Zhao, L. Luo, W. Zhang, H. Y. Jiang and J. Tang, *Appl. Catal., B*, 2020, **273**, 119054; https://doi.org/10.1016/j.apcatb.2020.119054.

18 C. Ferrara, A. Gentile, S. Marchionna, I. Quinzeni, M. Fracchia, P. Ghigna, S. Pollastri, C. Ritter, G. M. Vanacore and R. Ruffo, *Nano Lett.*, 2021, **21**, 8290; https://doi.org/10.1021/acs.nanolett.1C02809.

19 Y. Wu, J. Wu, C. Zhu, L. Zhang and J. Yan, *Chem. Eng. J.*, 2023, **465**, 142798; https://doi.org/10.1016/j.cej.2023.142798.

20 V. Natu, M. Benchakar, C. Canaff, A. Habrioux, S. Célérier and M. W. Barsoum, *Matter*, 2021, **4**, 1224; https://doi.org/10.1016/j.matt.2021.01.015.

21 L.-Å. Naslund, P. O. Å. Persson and J. Rosen, *J. Phys. Chem. C*, 2020, **124**, 27732; https://doi.org/10.1021/acs.jpcc.0C07413.

22 A. Tanvir, P. Sobolčiak, A. Popelka, M. Mrlik, Z. Spitalsky, M. Micusik, J. Prokes and I. Krupa, *Polymers*, 2019, **11**, 1272; https://doi.org/10.3390/polym11081272.

23 A. A. Saraev, A. Yu. Kurenkova, E. Yu. Gerasimov and E. A. Kozlova, *Nanomaterials*, 2022, **12**, 1584; https://doi.org/10.3390/nano12091584.

24 M. N. Lyulyukin, A. Yu. Kurenkova, A. V. Bukhtiyarov and E. A. Kozlova, *Mendeleev Commun.*, 2020, **30**, 192; https://doi.org/10.1016/j.mencom.2020.03.021.

25 Y. Xiao and W. Zhang, *Nanoscale*, 2020, **12**, 7660; https://doi.org/10.1039/C9NR10598K.

*Received: 8th July 2024; Com. 24/7588*